Measurement of $B_s^0 \to D_s^{(*)+} D_s^{(*)-}$ Branching Ratios

T. Aaltonen,[21] B. Álvarez González[z],[9] S. Amerio,[40] D. Amidei,[32] A. Anastassov[x],[15] A. Annovi,[17] J. Antos,[12] G. Apollinari,[15] J.A. Appel,[15] T. Arisawa,[54] A. Artikov,[13] J. Asaadi,[49] W. Ashmanskas,[15] B. Auerbach,[57] A. Aurisano,[49] F. Azfar,[39] W. Badgett,[15] T. Bae,[25] A. Barbaro-Galtieri,[26] V.E. Barnes,[44] B.A. Barnett,[23] P. Barria[hh],[42] P. Bartos,[12] M. Bauce[ff],[40] F. Bedeschi,[42] S. Behari,[23] G. Bellettini[gg],[42] J. Bellinger,[56] D. Benjamin,[14] A. Beretvas,[15] A. Bhatti,[46] D. Bisello[ff],[40] I. Bizjak,[28] K.R. Bland,[5] B. Blumenfeld,[23] A. Bocci,[14] A. Bodek,[45] D. Bortoletto,[44] J. Boudreau,[43] A. Boveia,[11] L. Brigliadori[ee],[6] C. Bromberg,[33] E. Brucken,[21] J. Budagov,[13] H.S. Budd,[45] K. Burkett,[15] G. Busetto[ff],[40] P. Bussey,[19] A. Buzatu,[31] A. Calamba,[10] C. Calancha,[29] S. Camarda,[4] M. Campanelli,[28] M. Campbell,[32] F. Canelli,[11, 15] B. Carls,[22] D. Carlsmith,[56] R. Carosi,[42] S. Carrillo[m],[16] S. Carron,[15] B. Casal[k],[9] M. Casarsa,[50] A. Castro[ee],[6] P. Catastini,[20] D. Cauz,[50] V. Cavaliere,[22] M. Cavalli-Sforza,[4] A. Cerri[f],[26] L. Cerrito[s],[28] Y.C. Chen,[1] M. Chertok,[7] G. Chiarelli,[42] G. Chlachidze,[15] F. Chlebana,[15] K. Cho,[25] D. Chokheli,[13] W.H. Chung,[56] Y.S. Chung,[45] M.A. Ciocci[hh],[42] A. Clark,[18] C. Clarke,[55] G. Compostella[ff],[40] M.E. Convery,[15] J. Conway,[7] M.Corbo,[15] M. Cordelli,[17] C.A. Cox,[7] D.J. Cox,[7] F. Crescioli[gg],[42] J. Cuevas[z],[9] R. Culbertson,[15] D. Dagenhart,[15] N. d'Ascenzo[w],[15] M. Datta,[15] P. de Barbaro,[45] M. Dell'Orso[gg],[42] L. Demortier,[46] M. Deninno,[6] F. Devoto,[21] M. d'Errico[ff],[40] A. Di Canto[gg],[42] B. Di Ruzza,[15] J.R. Dittmann,[5] M. D'Onofrio,[27] S. Donati[gg],[42] P. Dong,[15] M. Dorigo,[50] T. Dorigo,[40] K. Ebina,[54] A. Elagin,[49] A. Eppig,[32] R. Erbacher,[7] S. Errede,[22] N. Ershaidat[dd],[15] R. Eusebi,[49] S. Farrington,[39] M. Feindt,[24] J.P. Fernandez,[29] R. Field,[16] G. Flanagan[u],[15] R. Forrest,[7] M.J. Frank,[5] M. Franklin,[20] J.C. Freeman,[15] Y. Funakoshi,[54] I. Furic,[16] M. Gallinaro,[46] J.E. Garcia,[18] A.F. Garfinkel,[44] P. Garosi[hh],[42] H. Gerberich,[22] E. Gerchtein,[15] S. Giagu,[47] V. Giakoumopoulou,[3] P. Giannetti,[42] K. Gibson,[43] C.M. Ginsburg,[15] N. Giokaris,[3] P. Giromini,[17] G. Giurgiu,[23] V. Glagolev,[13] D. Glenzinski,[15] M. Gold,[35] D. Goldin,[49] N. Goldschmidt,[16] A. Golossanov,[15] G. Gomez,[9] G. Gomez-Ceballos,[30] M. Goncharov,[30] O. González,[29] I. Gorelov,[35] A.T. Goshaw,[14] K. Goulianos,[46] S. Grinstein,[4] C. Grosso-Pilcher,[11] R.C. Group[53],[15] J. Guimaraes da Costa,[20] S.R. Hahn,[15] E. Halkiadakis,[48] A. Hamaguchi,[38] J.Y. Han,[45] F. Happacher,[17] K. Hara,[51] D. Hare,[48] M. Hare,[52] R.F. Harr,[55] K. Hatakeyama,[5] C. Hays,[39] M. Heck,[24] J. Heinrich,[41] M. Herndon,[56] S. Hewamanage,[5] A. Hocker,[15] W. Hopkins[g],[15] D. Horn,[24] S. Hou,[1] R.E. Hughes,[36] M. Hurwitz,[11] U. Husemann,[57] N. Hussain,[31] M. Hussein,[33] J. Huston,[33] G. Introzzi,[42] M. Iori[jj],[47] A. Ivanov[p],[7] E. James,[15] D. Jang,[10] B. Jayatilaka,[14] E.J. Jeon,[25] S. Jindariani,[15] M. Jones,[44] K.K. Joo,[25] S.Y. Jun,[10] T.R. Junk,[15] T. Kamon[25],[49] P.E. Karchin,[55] A. Kasmi,[5] Y. Kato[o],[38] W. Ketchum,[11] J. Keung,[41] V. Khotilovich,[49] B. Kilminster,[15] D.H. Kim,[25] H.S. Kim,[25] J.E. Kim,[25] M.J. Kim,[17] S.B. Kim,[25] S.H. Kim,[51] Y.K. Kim,[11] Y.J. Kim,[25] N. Kimura,[54] M. Kirby,[15] S. Klimenko,[16] K. Knoepfel,[15] K. Kondo*,[54] D.J. Kong,[25] J. Konigsberg,[16] A.V. Kotwal,[14] M. Kreps[mm],[24] J. Kroll,[41] D. Krop,[11] M. Kruse,[14] V. Krutelyov[c],[49] T. Kuhr,[24] M. Kurata,[51] S. Kwang,[11] A.T. Laasanen,[44] S. Lami,[42] S. Lammel,[15] M. Lancaster,[28] R.L. Lander,[7] K. Lannon[y],[36] A. Lath,[48] G. Latino[hh],[42] T. LeCompte,[2] E. Lee,[49] H.S. Lee[q],[11] J.S. Lee,[25] S.W. Lee[bb],[49] S. Leo[gg],[42] S. Leone,[42] J.D. Lewis,[15] A. Limosani[t],[14] C.-J. Lin,[26] M. Lindgren,[15] E. Lipeles,[41] A. Lister,[18] D.O. Litvintsev,[15] C. Liu,[43] H. Liu,[53] Q. Liu,[44] T. Liu,[15] S. Lockwitz,[57] A. Loginov,[57] D. Lucchesi[ff],[40] J. Lueck,[24] P. Lujan,[26] P. Lukens,[15] G. Lungu,[46] J. Lys,[26] R. Lysak[e],[12] R. Madrak,[15] K. Maeshima,[15] P. Maestro[hh],[42] S. Malik,[46] G. Manca[a],[27] A. Manousakis-Katsikakis,[3] F. Margaroli,[47] C. Marino,[24] M. Martínez,[4] P. Mastrandrea,[47] K. Matera,[22] M.E. Mattson,[55] A. Mazzacane,[15] P. Mazzanti,[6] K.S. McFarland,[45] P. McIntyre,[49] R. McNulty[j],[27] A. Mehta,[27] P. Mehtala,[21] C. Mesropian,[46] T. Miao,[15] D. Mietlicki,[32] A. Mitra,[1] H. Miyake,[51] S. Moed,[15] N. Moggi,[6] M.N. Mondragon[m],[15] C.S. Moon,[25] R. Moore,[15] M.J. Morello[ii],[42] J. Morlock,[24] P. Movilla Fernandez,[15] A. Mukherjee,[15] Th. Muller,[24] P. Murat,[15] M. Mussini[ee],[6] J. Nachtman[n],[15] Y. Nagai,[51] J. Naganoma,[54] I. Nakano,[37] A. Napier,[52] J. Nett,[49] C. Neu,[53] M.S. Neubauer,[22] J. Nielsen[d],[26] L. Nodulman,[2] S.Y. Noh,[25] O. Norniella,[22] L. Oakes,[39] S.H. Oh,[14] Y.D. Oh,[25] I. Oksuzian,[53] T. Okusawa,[38] R. Orava,[21] L. Ortolan,[4] S. Pagan Griso[ff],[40] C. Pagliarone,[50] E. Palencia[f],[9] V. Papadimitriou,[15] A.A. Paramonov,[2] J. Patrick,[15] G. Pauletta[kk],[50] M. Paulini,[10] C. Paus,[30] D.E. Pellett,[7] A. Penzo,[50] T.J. Phillips,[14] G. Piacentino,[42] E. Pianori,[41] J. Pilot,[36] K. Pitts,[22] C. Plager,[8] L. Pondrom,[56] S. Poprocki[g],[15] K. Potamianos,[44] F. Prokoshin[cc],[13] A. Pranko,[26] F. Ptohos[h],[17] G. Punzi[gg],[42] A. Rahaman,[43] V. Ramakrishnan,[56] N. Ranjan,[44] I. Redondo,[29] P. Renton,[39] M. Rescigno,[47] T. Riddick,[28] F. Rimondi[ee],[6] L. Ristori[42],[15] A. Robson,[19] T. Rodrigo,[9] T. Rodriguez,[41] E. Rogers,[22] S. Rolli[i],[52] R. Roser,[15] F. Ruffini[hh],[42] A. Ruiz,[9] J. Russ,[10] V. Rusu,[15] A. Safonov,[49] W.K. Sakumoto,[45] Y. Sakurai,[54] L. Santi[kk],[50] K. Sato,[51] V. Saveliev[w],[15] A. Savoy-Navarro[aa],[15] P. Schlabach,[15] A. Schmidt,[24] E.E. Schmidt,[15] T. Schwarz,[15] L. Scodellaro,[9]

A. Scribano[hh,42] F. Scuri,[42] S. Seidel,[35] Y. Seiya,[38] A. Semenov,[13] F. Sforza[hh,42] S.Z. Shalhout,[7] T. Shears,[27] P.F. Shepard,[43] M. Shimojima[v,51] M. Shochet,[11] I. Shreyber-Tecker,[34] A. Simonenko,[13] P. Sinervo,[31] K. Sliwa,[52] J.R. Smith,[7] F.D. Snider,[15] A. Soha,[15] V. Sorin,[4] H. Song,[43] P. Squillacioti[hh,42] M. Stancari,[15] R. St. Denis,[19] B. Stelzer,[31] O. Stelzer-Chilton,[31] D. Stentz[x,15] J. Strologas,[35] G.L. Strycker,[32] Y. Sudo,[51] A. Sukhanov,[15] I. Suslov,[13] K. Takemasa,[51] Y. Takeuchi,[51] J. Tang,[11] M. Tecchio,[32] P.K. Teng,[1] J. Thom[g,15] J. Thome,[10] G.A. Thompson,[22] E. Thomson,[41] D. Toback,[49] S. Tokar,[12] K. Tollefson,[33] T. Tomura,[51] D. Tonelli,[15] S. Torre,[17] D. Torretta,[15] P. Totaro,[40] M. Trovato[ii,42] F. Ukegawa,[51] S. Uozumi,[25] A. Varganov,[32] F. Vázquez[m,16] G. Velev,[15] C. Vellidis,[15] M. Vidal,[44] I. Vila,[9] R. Vilar,[9] J. Vizán,[9] M. Vogel,[35] G. Volpi,[17] P. Wagner,[41] R.L. Wagner,[15] T. Wakisaka,[38] R. Wallny,[8] S.M. Wang,[1] A. Warburton,[31] D. Waters,[28] W.C. Wester III,[15] D. Whiteson[b,41] A.B. Wicklund,[2] E. Wicklund,[15] S. Wilbur,[11] F. Wick,[24] H.H. Williams,[41] J.S. Wilson,[36] P. Wilson,[15] B.L. Winer,[36] P. Wittich[g,15] S. Wolbers,[15] H. Wolfe,[36] T. Wright,[32] X. Wu,[18] Z. Wu,[5] K. Yamamoto,[38] D. Yamato,[38] T. Yang,[15] U.K. Yang[r,11] Y.C. Yang,[25] W.-M. Yao,[26] G.P. Yeh,[15] K. Yi[n,15] J. Yoh,[15] K. Yorita,[54] T. Yoshida[l,38] G.B. Yu,[14] I. Yu,[25] S.S. Yu,[15] J.C. Yun,[15] A. Zanetti,[50] Y. Zeng,[14] C. Zhou,[14] and S. Zucchelli[ee6]

(CDF Collaboration[†])

[1]Institute of Physics, Academia Sinica, Taipei, Taiwan 11529, Republic of China
[2]Argonne National Laboratory, Argonne, Illinois 60439, USA
[3]University of Athens, 157 71 Athens, Greece
[4]Institut de Fisica d'Altes Energies, ICREA, Universitat Autonoma de Barcelona, E-08193, Bellaterra (Barcelona), Spain
[5]Baylor University, Waco, Texas 76798, USA
[6]Istituto Nazionale di Fisica Nucleare Bologna, [ee]University of Bologna, I-40127 Bologna, Italy
[7]University of California, Davis, Davis, California 95616, USA
[8]University of California, Los Angeles, Los Angeles, California 90024, USA
[9]Instituto de Fisica de Cantabria, CSIC-University of Cantabria, 39005 Santander, Spain
[10]Carnegie Mellon University, Pittsburgh, Pennsylvania 15213, USA
[11]Enrico Fermi Institute, University of Chicago, Chicago, Illinois 60637, USA
[12]Comenius University, 842 48 Bratislava, Slovakia; Institute of Experimental Physics, 040 01 Kosice, Slovakia
[13]Joint Institute for Nuclear Research, RU-141980 Dubna, Russia
[14]Duke University, Durham, North Carolina 27708, USA
[15]Fermi National Accelerator Laboratory, Batavia, Illinois 60510, USA
[16]University of Florida, Gainesville, Florida 32611, USA
[17]Laboratori Nazionali di Frascati, Istituto Nazionale di Fisica Nucleare, I-00044 Frascati, Italy
[18]University of Geneva, CH-1211 Geneva 4, Switzerland
[19]Glasgow University, Glasgow G12 8QQ, United Kingdom
[20]Harvard University, Cambridge, Massachusetts 02138, USA
[21]Division of High Energy Physics, Department of Physics,
University of Helsinki and Helsinki Institute of Physics, FIN-00014, Helsinki, Finland
[22]University of Illinois, Urbana, Illinois 61801, USA
[23]The Johns Hopkins University, Baltimore, Maryland 21218, USA
[24]Institut für Experimentelle Kernphysik, Karlsruhe Institute of Technology, D-76131 Karlsruhe, Germany
[25]Center for High Energy Physics: Kyungpook National University,
Daegu 702-701, Korea; Seoul National University, Seoul 151-742,
Korea; Sungkyunkwan University, Suwon 440-746,
Korea; Korea Institute of Science and Technology Information,
Daejeon 305-806, Korea; Chonnam National University, Gwangju 500-757,
Korea; Chonbuk National University, Jeonju 561-756, Korea
[26]Ernest Orlando Lawrence Berkeley National Laboratory, Berkeley, California 94720, USA
[27]University of Liverpool, Liverpool L69 7ZE, United Kingdom
[28]University College London, London WC1E 6BT, United Kingdom
[29]Centro de Investigaciones Energeticas Medioambientales y Tecnologicas, E-28040 Madrid, Spain
[30]Massachusetts Institute of Technology, Cambridge, Massachusetts 02139, USA
[31]Institute of Particle Physics: McGill University, Montréal, Québec,
Canada H3A 2T8; Simon Fraser University, Burnaby, British Columbia,
Canada V5A 1S6; University of Toronto, Toronto, Ontario,
Canada M5S 1A7; and TRIUMF, Vancouver, British Columbia, Canada V6T 2A3
[32]University of Michigan, Ann Arbor, Michigan 48109, USA
[33]Michigan State University, East Lansing, Michigan 48824, USA
[34]Institution for Theoretical and Experimental Physics, ITEP, Moscow 117259, Russia
[35]University of New Mexico, Albuquerque, New Mexico 87131, USA
[36]The Ohio State University, Columbus, Ohio 43210, USA
[37]Okayama University, Okayama 700-8530, Japan

^{38}Osaka City University, Osaka 588, Japan
^{39}University of Oxford, Oxford OX1 3RH, United Kingdom
^{40}Istituto Nazionale di Fisica Nucleare, Sezione di Padova-Trento, ^{ff}University of Padova, I-35131 Padova, Italy
^{41}University of Pennsylvania, Philadelphia, Pennsylvania 19104, USA
^{42}Istituto Nazionale di Fisica Nucleare Pisa, ^{gg}University of Pisa,
^{hh}University of Siena and ^{ii}Scuola Normale Superiore, I-56127 Pisa, Italy
^{43}University of Pittsburgh, Pittsburgh, Pennsylvania 15260, USA
^{44}Purdue University, West Lafayette, Indiana 47907, USA
^{45}University of Rochester, Rochester, New York 14627, USA
^{46}The Rockefeller University, New York, New York 10065, USA
^{47}Istituto Nazionale di Fisica Nucleare, Sezione di Roma 1,
^{jj}Sapienza Università di Roma, I-00185 Roma, Italy
^{48}Rutgers University, Piscataway, New Jersey 08855, USA
^{49}Texas A&M University, College Station, Texas 77843, USA
^{50}Istituto Nazionale di Fisica Nucleare Trieste/Udine,
I-34100 Trieste, ^{kk}University of Udine, I-33100 Udine, Italy
^{51}University of Tsukuba, Tsukuba, Ibaraki 305, Japan
^{52}Tufts University, Medford, Massachusetts 02155, USA
^{53}University of Virginia, Charlottesville, Virginia 22906, USA
^{54}Waseda University, Tokyo 169, Japan
^{55}Wayne State University, Detroit, Michigan 48201, USA
^{56}University of Wisconsin, Madison, Wisconsin 53706, USA
^{57}Yale University, New Haven, Connecticut 06520, USA
(Dated: March 2, 2013)

The decays $B_s^0 \to D_s^{(*)+} D_s^{(*)-}$ are reconstructed in a data sample corresponding to an integrated luminosity of 6.8 fb^{-1} collected by the CDF II detector at the Tevatron $p\bar{p}$ collider. All decay modes are observed with a significance of more than $10\,\sigma$, and we measure the B_s^0 production rate times $B_s^0 \to D_s^{(*)+} D_s^{(*)-}$ branching ratios relative to the normalization mode $B^0 \to D_s^+ D^-$ to be $0.183 \pm 0.021 \pm 0.017$ for $B_s^0 \to D_s^+ D_s^-$, $0.424 \pm 0.046 \pm 0.035$ for $B_s^0 \to D_s^{*\pm} D_s^{\mp}$, $0.654 \pm 0.072 \pm 0.065$ for $B_s^0 \to D_s^{*+} D_s^{*-}$, and $1.261 \pm 0.095 \pm 0.112$ for the inclusive decay $B_s^0 \to D_s^{(*)+} D_s^{(*)-}$, where the uncertainties are statistical and systematic. These results are the most precise single measurements to date and provide important constraints for indirect searches for non-standard model physics in B_s^0 mixing.

PACS numbers: 13.25.Hw, 14.40.Nd, 12.15.Ff

*Deceased
†With visitors from ^{a}Istituto Nazionale di Fisica Nucleare, Sezione di Cagliari, 09042 Monserrato (Cagliari), Italy, ^{b}University of CA Irvine, Irvine, CA 92697, USA, ^{c}University of CA Santa Barbara, Santa Barbara, CA 93106, USA, ^{d}University of CA Santa Cruz, Santa Cruz, CA 95064, USA, ^{e}Institute of Physics, Academy of Sciences of the Czech Republic, Czech Republic, ^{f}CERN, CH-1211 Geneva, Switzerland, ^{g}Cornell University, Ithaca, NY 14853, USA, ^{h}University of Cyprus, Nicosia CY-1678, Cyprus, ^{i}Office of Science, U.S. Department of Energy, Washington, DC 20585, USA, ^{j}University College Dublin, Dublin 4, Ireland, ^{k}ETH, 8092 Zurich, Switzerland, ^{l}University of Fukui, Fukui City, Fukui Prefecture, Japan 910-0017, ^{m}Universidad Iberoamericana, Mexico D.F., Mexico, ^{n}University of Iowa, Iowa City, IA 52242, USA, ^{o}Kinki University, Higashi-Osaka City, Japan 577-8502, ^{p}Kansas State University, Manhattan, KS 66506, USA, ^{q}Ewha Womans University, Seoul, 120-750, Korea, ^{r}University of Manchester, Manchester M13 9PL, United Kingdom, ^{s}Queen Mary, University of London, London, E1 4NS, United Kingdom, ^{t}University of Melbourne, Victoria 3010, Australia, ^{u}Muons, Inc., Batavia, IL 60510, USA, ^{v}Nagasaki Institute of Applied Science, Nagasaki, Japan, ^{w}National Research Nuclear University, Moscow, Russia, ^{x}Northwestern University, Evanston, IL 60208, USA, ^{y}University of Notre Dame, Notre Dame, IN 46556, USA, ^{z}Universidad de Oviedo, E-33007 Oviedo, Spain, ^{aa}CNRS-IN2P3, Paris, F-75205 France, ^{bb}Texas Tech University,

Lubbock, TX 79609, USA, ^{cc}Universidad Tecnica Federico Santa Maria, 110v Valparaiso, Chile, ^{dd}Yarmouk University, Irbid 211-63, Jordan, ^{mm}University of Warwick, Coventry CV4 7AL, United Kingdom,

A B_s^0 meson can oscillate into its antiparticle via second order weak interaction transitions, which make its time evolution sensitive to contributions from new physics processes. Such contributions are not well constrained yet and might be responsible for the deviation from the standard model reported in Ref. [1]. The B_s^0 eigenstates with defined mass and lifetime, B_{sL}^0 and B_{sH}^0, are linear combinations of the B_s^0 and $\bar{B}_s^0$ states and, in the standard model, correspond in good approximation to the even and odd CP eigenstates, respectively. In the absence of substantial CP violation, a sizable decay width difference between the light and heavy mass eigenstates, $\Delta\Gamma_s = \Gamma_{sL} - \Gamma_{sH}$, arises from the fact that decays to final states of definite CP are only accessible by one of the mass eigenstates. The dominant contribution to $\Delta\Gamma_s$ is believed to come from the $B_s^0 \to D_s^{(*)+} D_s^{(*)-}$ de-

cays [2], which are predominantly CP-even and saturate $\Delta\Gamma_s$ under certain theoretical assumptions [3, 4], resulting in the relation

$$2\mathcal{B}(B_s^0 \to D_s^{(*)+}D_s^{(*)-}) \approx \frac{\Delta\Gamma_s}{\Gamma_s + \Delta\Gamma_s/2}, \qquad (1)$$

where $\Gamma_s = (\Gamma_{sL} + \Gamma_{sH})/2$ [5]. However, three-body modes may provide a significant contribution to $\Delta\Gamma_s$ [6].

A finite value of $\Delta\Gamma_s$ improves the experimental sensitivity to CP violation because it allows one to distinguish the two mass eigenstates via their decay time distribution. Furthermore, the $B_s^0 \to D_s^{(*)+}D_s^{(*)-}$ decays could be used in future to measure directly the lifetime of the CP-even eigenstate, which would complement the CP-odd eigenstate lifetime measurement in $B_s^0 \to J/\psi f_0(980)$ decays [7] and provide additional information in the search for new physics contributions to CP violation in the B_s^0 system.

The $B_s^0 \to D_s^{(*)+}D_s^{(*)-}$ decay modes have been previously studied by the ALEPH, CDF, D0, and Belle collaborations [8–11]. The current world average branching ratios [12], which do not yet include the latest preliminary Belle results [13], are $\mathcal{B}(B_s^0 \to D_s^+ D_s^-) = (1.04^{+0.29}_{-0.26})\,\%$, $\mathcal{B}(B_s^0 \to D_s^{*\pm}D_s^{\mp}) = (2.8 \pm 1.0)\,\%$, $\mathcal{B}(B_s^0 \to D_s^{*+}D_s^{*-}) = (3.1 \pm 1.4)\,\%$, and $\mathcal{B}(B_s^0 \to D_s^{(*)+}D_s^{(*)-}) = (4.5 \pm 1.4)\,\%$.

In a data sample corresponding to an integrated luminosity of 6.8 fb^{-1} recorded by the CDF II detector at the Tevatron $p\bar{p}$ collider we reconstruct $B_s^0 \to D_s^{(*)+}D_s^{(*)-}$ decays with $D_s^+ \to K^+K^-\pi^+$. For the first time in this channel, the acceptance is calculated using a $D_s^{\pm}$ Dalitz model instead of a simple two-body decay model. The photon and the neutral pion from the $D_s^{*+} \to D_s^+\gamma$ and $D_s^{*+} \to D_s^+\pi^0$ decays are not reconstructed because of their low detection efficiency. In a simultaneous fit to the reconstructed $B_{(s)}^0$ meson invariant mass spectra we measure the B_s^0 production rate times $B_s^0 \to D_s^{(*)+}D_s^{(*)-}$ branching ratios relative to the normalization mode $B^0 \to D_s^+D^-$

$$f_X = \frac{f_s}{f_d} \frac{\mathcal{B}(B_s^0 \to X)}{\mathcal{B}(B^0 \to D_s^+D^-)}, \qquad (2)$$

for $X = D_s^+D_s^-$, $D_s^{*\pm}D_s^{\mp}$, $D_s^{*+}D_s^{*-}$, and the inclusive $D_s^{(*)+}D_s^{(*)-}$ where f_s/f_d is the relative rate of produced B_s^0 to B^0 mesons.

The components of the CDF II detector [14] most relevant for this analysis are the tracking systems located inside a solenoid that provides a 1.4 T magnetic field. Charged particles' trajectories (tracks) are reconstructed in layers of silicon-strip sensors located between radii of 1.5 cm and 28 cm from the beam line and an open-cell drift chamber (COT) with a radial extension from 40 to 137 cm. Tracks with a pseudorapidity $|\eta| \leq 1.0$ pass the full radial extent of the COT. Kaons and pions are statistically identified by measurements of the ionization

energy loss in the COT and information from the time-of-flight system located between the COT and the solenoid. The events for this analysis are selected online by identifying pairs of tracks detected in the COT and the silicon detector [15]. Minimal requirements on the momenta and the displacement of the tracks and the reconstructed decay vertex from the primary vertex are imposed.

We reconstruct $D_s^+ \to K^+K^-\pi^+$ and $D^+ \to K^-\pi^+\pi^+$ decays from combinations of three tracks with appropriate charge and mass hypothesis assignments, fitted to a common vertex. Because the $D_s^+ \to K^+K^-\pi^+$ decay proceeds mainly via $\phi\pi^+$ and $\bar{K}^{*0}K^+$, we select candidates with $1.005 < m(K^+K^-) < 1.035$ GeV/c^2 and $0.837 < m(K^-\pi^+) < 0.947$ GeV/c^2, centered on the known ϕ and K^{*0} masses, respectively. According to the $D_s^+ \to K^+K^-\pi^+$ Dalitz structure [16] this requirement has a signal acceptance of about 75 % while covering only 14 % of the phase space and thus increasing the signal-to-background ratio. In the following we will denote the selected K^+K^- and $K^-\pi^+$ combinations as ϕ and $\bar{K}^{*0}$, respectively, since the dominant contributions come from these resonances. However, we implicitly include contributions from other resonances and interference effects when using these terms.

Pairs of $D_s^+ \to \phi\pi^+$ or $D_s^+ \to \bar{K}^{*0}K^+$ candidates and $D_s^- \to \phi\pi^-$ candidates are combined to form B_s^0 candidates and fitted to a common vertex. Combinations where both charm mesons decay into a $\bar{K}^{*0}$ mode are not considered because of the low signal-to-background ratio. Candidate B^0 mesons are reconstructed from $D_s^+D^-$ combinations where both D_s^+ decay modes are used.

To reject background-like events, requirements are placed on track quality variables, B meson momentum, reconstructed D meson masses, vertex fit qualities, and vertex displacement significances. To further increase the signal purity, two artificial neural networks are used, one for candidates with a $\bar{K}^{*0}$ and one for candidates without. To minimize the systematic uncertainty of the relative selection efficiency, the same networks are applied to B_s^0 and B^0 candidates, and only information from the $D_s^{\pm}$ that is common to both B meson decays is used. The networks are trained on simulated signal events, described below, and on background events from the 5.45 to 6.5 GeV/c^2 B mass sideband. The input variables contain kinematic, lifetime, fit quality, and particle identification information. The B vertex displacement significance in the transverse plane gives the largest contribution to the discrimination power of both networks. The selection criteria on the network outputs are chosen such that they maximize the significance $\epsilon_{\mathrm{MC}}/\sqrt{N_{\mathrm{data}}}$, where ϵ_{MC} is the B_s^0 selection efficiency determined from simulation and N_{data} is the number of data events in the B_s^0 signal window from 5.343 to 5.397 GeV/c^2.

About 6 % of the selected $B^0 \to D_s^+(\to \phi\pi^+)D^-$ candidates also fulfill the B_s^0 selection requirements, where the assignment of a D^- daughter track is swapped from

pion to kaon. To avoid having the same event entering the fit multiple times, we reject each event that is reconstructed as B_s^0 candidates from the B^0 sample. The cross-populations between the two B_s^0 modes and between the two B^0 modes, respectively, are negligible. The selected sample contains about 750 B_s^0 signal events.

Simulated events are used to determine the reconstruction and selection efficiency. The $B_{(s)}^0$ mesons are generated according to the momentum spectrum measured in exclusive B decays and decayed to the considered final states with the EVTGEN package [17]. For the B_s^0 meson we assign the lifetime of the B_{sL}^0 eigenstate [12] that coincides with the CP-even eigenstate in the standard model. For all the other long-lived charm and bottom mesons, the world average mean lifetimes [12] are used. The $B_s^0 \to D_s^{*+} D_s^{*-}$ decay is a transition of a pseudoscalar to two vector mesons and its angular distribution is described by three polarization amplitudes. Since these amplitudes are unknown, we take the same longitudinal polarization as measured in $B^0 \to D^{*+} D^{*-}$ decays [18] and a vanishing CP-odd component as default values. The world average value [12] is used for the ratio of $D_s^{*+} \to D_s^+ \gamma$ to $D_s^{*+} \to D_s^+ \pi^0$ decays. The dynamics of the decay $D_s^+ \to K^+ K^- \pi^+$ is simulated according to the Dalitz structure measured by CLEO [16]. The generated events are processed by a GEANT3 based detector simulation [19] and the same reconstruction program as applied to real data events.

The relative branching ratios times production rate are determined in a simultaneous extended unbinned maximum-likelihood fit to the $(\phi\pi^+)(\phi\pi^-)$, $(\bar{K}^{*0}K^+)(\phi\pi^-)$, $(\phi\pi^+)(K^+\pi^-\pi^-)$, and $(\bar{K}^{*0}K^+)(K^+\pi^-\pi^-)$ invariant mass distributions. By simultaneously fitting all four distributions, the normalization of the B^0 reflections in the $(\bar{K}^{*0}K^+)(\phi\pi^-)$ spectrum is constrained by the yields in the high-statistics $(\phi\pi^+)(K^+\pi^-\pi^-)$ sample. The components of the fit function for each invariant mass distribution are fully and partially reconstructed signals, reflections, and background. The fully reconstructed B_s^0 and B^0 signals are parametrized by the sum of two Gaussians with relative normalizations and widths derived from simulation. To account for discrepancies between data and simulation, a factor is introduced for the B_s^0 and B^0 signal shapes, respectively, that scales the widths of the Gaussians and that is allowed to float in the fit. The shapes of partially reconstructed signal events and of reflections from $B^0 \to (\phi\pi^+)(K^+\pi^-\pi^-)$ mis-reconstructed as $B_s^0 \to (\phi\pi^+)(K^{*0}K^-)$ are determined from simulation using empirical models. Background from random combinations of tracks and other B decays is described by an exponential plus a constant function with all parameters floated in the fit.

The yield of fully reconstructed B^0 mesons in the final state i, $(\phi\pi^+)(K^+\pi^-\pi^-)$ or $(\bar{K}^{*0}K^+)(K^+\pi^-\pi^-)$, is

given by

$$N_{\text{rec},i}^{B^0} = N_{\text{tot}}^{B^0} \mathcal{B}(B^0 \to D_s^+ D^-) \mathcal{B}(D_s^+ \to K^+ K^- \pi^+)$$
$$\cdot \mathcal{B}(D^+ \to K^- \pi^+ \pi^+) \epsilon_i^{B^0}, \qquad (3)$$

where $N_{\text{tot}}^{B^0}$ is the total number of produced B^0 mesons and is a free parameter in the fit, the branching ratios are taken from Ref. [12], and the efficiency $\epsilon_i^{B^0}$ is determined from simulation. Equivalent expressions are used for the yields of partially reconstructed B^0 decays with an additional branching ratio factor for the D^{*+} and D_s^{*+} decays. The normalizations of reflections are calculated in the same way, but with the efficiencies replaced by the mis-reconstruction fractions determined from simulation. The number of fully reconstructed B_s^0 mesons in the final state i, $(\phi\pi^+)(\phi\pi^-)$ or $(\bar{K}^{*0}K^+)(\phi\pi^-)$, where the D_s^+ decays in the same mode as the D_s^+ from the B^0 decay is given by

$$N_{\text{rec},i}^{B_s^0} = N_{\text{rec},i}^{B^0} f_{D_s D_s} \frac{\mathcal{B}(D_s^+ \to K^+ K^- \pi^+)}{\mathcal{B}(D^+ \to K^- \pi^+ \pi^+)} \frac{\epsilon_i^{B_s^0}}{\epsilon_i^{B^0}}, \qquad (4)$$

with $f_{D_s D_s}$ as a free parameter and $N_{\text{rec},i}^{B^0}$ given by Eq. (3). Equivalent equations hold for partially reconstructed B_s^0 decays.

Projections of the fit result are compared to the distribution of data events in Fig. 1. The statistical significance of each signal exceeds $10\,\sigma$ as estimated from a likelihood ratio of the fit with and without the signal component.

Systematic uncertainties on the fitted signal yields arise from the signal and background models. Because the width scale factors of the fully reconstructed signal components are allowed to float in the fit, the systematic uncertainties of these components are already included in the statistical errors. To estimate the systematic effect due to the fixed shapes of the partially reconstructed signal components and reflections, we repeat the fit multiple times with shape parameters randomly varied according to the covariance matrix of the fits of the shapes to simulated data. The mean deviations with respect to the central values are assigned as systematic uncertainties. The systematic uncertainties due to the background mass model are estimated from the changes in the results caused by using a second order polynomial instead of the sum of an exponential and a constant function. By applying the selection optimization procedure on the normalization instead of the signal mode we verified that a possible selection bias is negligible.

Systematic effects in the relative efficiency determination can be caused by a simulation that does not describe the data accurately. One source of systematic uncertainties is the trigger simulation, which can lead to a discrepancy in the B meson momentum spectrum. Although this effect cancels to first order in the ratio measurement, it is accounted for by a reweighting of the simulated
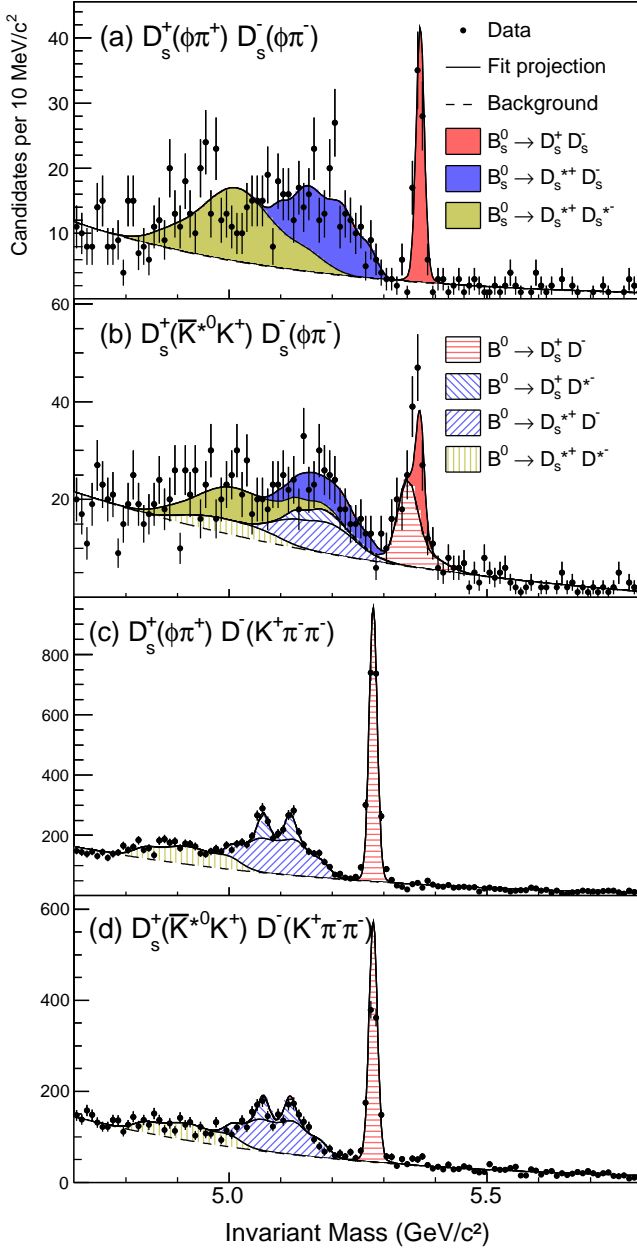
FIG. 1: Invariant mass distribution of (a) $B_s^0 \to D_s^+(\phi\pi^+)D_s^-(\phi\pi^-)$, (b) $B_s^0 \to D_s^+(\bar{K}^{*0}K^+)D_s^-(\phi\pi^-)$, (c) $B^0 \to D_s^+(\phi\pi^+)D^-(K^+\pi^-\pi^-)$, and (d) $B^0 \to D_s^+(\bar{K}^{*0}K^+)D^-(K^+\pi^-\pi^-)$ candidates with the simultaneous fit projection overlaid. The broader structures stem from decays where the photon or π^0 from the $D_{(s)}^{*+}$ decay is not reconstructed. Misreconstructed signal events in (c) show up as reflections in (b).

events. The systematic uncertainties due to the detector simulation are estimated by the shift of the results with respect to the case in which this reweighting is not applied. The uncertainties on the world average B^0, D^+, and D_s^+ lifetimes are propagated by varying the lifetimes in the simulation. For the B_s^0 lifetime, we consider two

Source	$f_{D_sD_s}$	$f_{D_s^*D_s}$	$f_{D_s^*D_s^*}$	$f_{D_s^{(*)}D_s^{(*)}}$
Signal model	0.003	0.007	0.009	0.019
Background model	0.001	0.004	0.030	0.033
Detector simulation	0.001	0.003	0.010	0.005
B, D lifetimes	$+0.001$ -0.002	$+0.002$ -0.004	$+0.003$ -0.006	$+0.006$ -0.012
Dalitz model	0.011	0.024	0.038	0.073
Helicity model	0.001	0.005	0.012	0.008
Branching fractions	0.013	0.024	0.039	0.074
Total	0.017	0.035	0.065	0.112

TABLE I: Overview of systematic uncertainties on the measured ratios of branching fractions.

cases, the 1σ lower bound of the world average short-lived eigenstate lifetime and the 1σ upper bound of the mean B_s^0 lifetime. The effects on the acceptance induced by variations of the $D_s^+ \to K^+K^-\pi^+$ Dalitz structure are considered by generating different Dalitz model scenarios, with Dalitz model parameter values varied according to the systematic and correlated statistical uncertainties of the CLEO Dalitz fit. The uncertainties of the D^+ Dalitz model have a negligible effect on the result. For $B_s^0 \to D_s^{*+}D_s^{*-}$ decays we investigate the effects of both a longitudinal polarization fraction f_L deviating from our nominal assumption and a non-zero fraction of the CP-odd component f_{CP-}. The fraction f_L is varied in the simulation according to the uncertainty of the f_L measurement in $B^0 \to D^{*+}D^{*-}$ decays [18]. A variation of f_{CP-} shows no effect on the $B_s^0 \to D_s^{*+}D_s^{*-}$ mass line shape, fit quality, or measured branching fraction ratios. The effect of self cross-feed due to a wrong assignment of kaon and pion masses is negligible.

Further systematic uncertainties arise from external input quantities. The uncertainties of intermediate and final state branching fractions, $\mathcal{B}(D_s^+ \to K^+K^-\pi^+)$, $\mathcal{B}(D^+ \to K^-\pi^+\pi^+)$, and $\mathcal{B}(D^{*+} \to D^+\gamma/\pi^0)$, are propagated in the fit by adding Gaussian constraints to the corresponding fit parameters. The resulting uncertainties of the measured branching fraction ratios are extracted by subtracting in quadrature the statistical uncertainties of the fits with branching fraction constrained and the one where they are fixed to the central values. When calculating the absolute branching fractions $\mathcal{B}(B_s^0 \to D_s^{(*)+}D_s^{(*)-})$ an additional relative uncertainty of 16 % is introduced by the measurement uncertainties of f_s/f_d and the branching fraction of the normalization channel $B^0 \to D_s^+D^-$. The systematic uncertainties are summarized in Table I.

As a result we obtain $f_{D_sD_s} = 0.183 \pm 0.021 \pm 0.017$, $f_{D_s^*D_s} = 0.424 \pm 0.046 \pm 0.035$, $f_{D_s^*D_s^*} = 0.654 \pm 0.072 \pm 0.065$, and $f_{D_s^{(*)}D_s^{(*)}} = 1.261 \pm 0.095 \pm 0.112$, where the first uncertainties are statistical and the second systematic. Taking $\mathcal{B}(B^0 \to D_s^+D^-) = (7.2 \pm 0.8) \times 10^{-3}$ from Ref. [12] and $f_s/f_d = 0.269 \pm 0.033$ from Ref. [12, 20] an absolute inclusive branching ratio of

$\mathcal{B}(B_s^0 \to D_s^{(*)+} D_s^{(*)-}) = (3.38 \pm 0.25 \pm 0.30 \pm 0.56)\,\%$ is calculated where the third uncertainty comes from the normalization. Assuming Eq. (1) to hold this would translate into a decay width difference contribution of the $B_s^0 \to D_s^{(*)+} D_s^{(*)-}$ modes of $\Delta\Gamma_s/\Gamma_s = (6.99 \pm 0.54 \pm 0.64 \pm 1.20)\,\%$, which is consistent with the standard model expectation [21].

In summary, we have measured the branching ratios of $B_s^0 \to D_s^+ D_s^-$, $B_s^0 \to D_s^{*\pm} D_s^{\mp}$, $B_s^0 \to D_s^{*+} D_s^{*-}$, and $B_s^0 \to D_s^{(*)+} D_s^{(*)-}$ decays relative to the normalization mode $B^0 \to D_s^+ D^-$. Compared to previous analyses, we have reduced the systematic uncertainties by taking into account the full $D_s^+ \to K^+ K^- \pi^+$ Dalitz structure, as opposed to using a simple two-body D_s^+ decay model. The derived absolute branching ratios of $\mathcal{B}(B_s^0 \to D_s^+ D_s^-) = (0.49 \pm 0.06 \pm 0.05 \pm 0.08)\,\%$, $\mathcal{B}(B_s^0 \to D_s^{*\pm} D_s^{\mp}) = (1.13 \pm 0.12 \pm 0.09 \pm 0.19)\,\%$, $\mathcal{B}(B_s^0 \to D_s^{*+} D_s^{*-}) = (1.75 \pm 0.19 \pm 0.17 \pm 0.29)\,\%$, and $\mathcal{B}(B_s^0 \to D_s^{(*)+} D_s^{(*)-}) = (3.38 \pm 0.25 \pm 0.30 \pm 0.56)\,\%$, where the uncertainties are statistical, systematic, and due to the normalization, are the most precise measurements to date. The central values are lower than but consistent with the Belle result [11] and the previous CDF result, which is superseded by this measurement.

---

[1] V. M. Abazov *et al.* (D0 Collaboration), Phys. Rev. D **84**, 052007 (2011).

[2] Charge-conjugate modes are implicitly included throughout this paper.

[3] R. Aleksan *et al.*, Phys. Lett. B **316**, 567 (1993).

[4] M. A. Shifman and M. B. Voloshin, Yad. Fiz. **47**, 801 (1988) [Sov. J. Nucl. Phys. **47**, 511 (1988)].

[5] I. Dunietz, R. Fleischer and U. Nierste, Phys. Rev. D **63**, 114015 (2001).

[6] C. K. Chua, W. S. Hou, and C. H. Shen, Phys. Rev. D **84**, 074037 (2011).

[7] T. Aaltonen *et al.* (CDF Collaboration), Phys. Rev. D **84**, 052012 (2011).

[8] R. Barate *et al.* (ALEPH Collaboration), Phys. Lett. B **486**, 286 (2000).

[9] T. Aaltonen *et al.* (CDF Collaboration), Phys. Rev. Lett. **100**, 021803 (2008).

[10] V. M. Abazov *et al.* (D0 Collaboration), Phys. Rev. Lett. **102**, 091801 (2009).

[11] S. Esen *et al.* (Belle Collaboration), Phys. Rev. Lett. **105**, 201802 (2010).

[12] K. Nakamura *et al.* (Particle Data Group), J. Phys. G **37**, 075021 (2010), and 2011 partial update.

[13] S. Esen, arXiv:hep-ex/1110.2099.

[14] D. E. Acosta *et al.* (CDF Collaboration), Phys. Rev. D **71**, 032001 (2005).

[15] E. J. Thomson *et al.*, IEEE Trans. Nucl. Sci., **49**, 1063 (2002); B. Ashmanskas *et al.*, Nucl. Instrum. Methods A **518**, 532 (2004); L. Ristori and G. Punzi, Ann. Rev. Nucl. Part. Sci **60**, 595 (2010).

[16] R. E. Mitchell *et al.* (CLEO Collaboration), Phys. Rev. D **79**, 072008 (2009).

[17] D. Lange, Nucl. Instrum. Methods A **462**, 152 (2001).

[18] B. Aubert *et al.* (BaBar Collaboration), Phys. Rev. D **67**, 092003 (2003).

[19] R. Brun, R. Hagelberg, M. Hansroul, and J. Lassalle, CERN-DD-78-2-REV, 1978 (unpublished).

[20] T. Aaltonen *et al.* (CDF Collaboration), Phys. Rev. D **77**, 072003 (2008).

[21] A. Lenz and U. Nierste, J. High Energy Phys. **0706**, 072 (2007); arXiv:1102.4274 [hep-ph].